Supplement of Atmos. Chem. Phys., 14, 9171–9200, 2014
http://www.atmos-chem-phys.net/14/9171/2014/
doi:10.5194/acp-14-9171-2014-supplement

Atmospheric Chemistry and Physics
Open Access

Supplement of

Improvement and further development in CESM/CAM5: gas-phase chemistry and inorganic aerosol treatments

J. He and Y. Zhang

Correspondence to: Y. Zhang (yang_zhang@ncsu.edu)

1. Datasets for model evaluation

A number of observational datasets from surface networks and satellites are used for model evaluation. They are summarized along with the variables to be evaluated in Table S1.

2. The Student's t-Test

To determine if the changes in model predictions due to changes in model configurations are statistically significant, the student's t-test analysis is performed between six pairs of 2001 simulations with different model configurations. Table S2 summarizes those results. The results show that the changes in most cloud/radiative variables due to changes in model configurations are statistically significant.

3. Performance Statistics for JJA from the 2001-2005 Simulations

As shown in Table S3, MAM_NEW_5YA improves performance of radiative variables such as LWD, SWD, and OLR with reduced absolute values of NMB, NME, and RMSE during June, July, and August (JJA) of 2001-2005, although it slightly degrades the performance of SWCF. MAM_NEW_5YA also improves cloud variables such as CF, COT, CWP, CCN5, and CDNC, with absolute reduction of NMBs of 0.9-18.0%. As shown in Table S4, with all new and modified treatments in MAM_NEW_5YA, SO_4^{2-}, BC, OC, TC, and PM_{25} are improved over CONUS, SO_4^{2-}, PM_{25}, and PM_{10} are improved over Europe, and SO_2 and PM_{10} are improved over East Asia, and TOR is improved over globe. Compared with full 5-year (2001-2005) average (ANU), JJA gives better model predictions for radiation (e.g., LWD, SWD, and OLR) and cloud (e.g., COT, CWP, column CCN5, and CDNC).

4. Impacts of Gas-Aerosol Partitioning

The chemical regimes is the controlling factor for gas-aerosol equilibrium partitioning, which is determined based on the ratio of SO_4^{2-} molar concentrations to total molar concentrations of cations and their respective gases (referred to as TCAT/TSO4) (Zhang et al., 2000). Three regimes are defined based on the values of TCAT/TSO4: (1) if TCAT/TSO4 < 2, the system contains excess sulfate and is in a sulfate-rich regime; (2) if TCAT/TSO4 = 2, the system contains just sufficient sulfate to neutralize the cation species and is in sulfate-neutral regime; (3) if TCAT/TSO4 > 2, the system contain insufficient sulfate to neutralize the cation species and is in sulfate-poor regime. Over land, the major cation is NH_4^+, and there are also crustal species (K^+, Ca^{2+}, and Mg^{2+}) associated with dust emissions, whereas over ocean, the major cation is Na^+, which is a non-volatile species. Therefore, the gas-aerosol equilibrium partitioning behaves differently over land and over ocean. Figure S1 shows the absolute differences of H_2SO_4, fine particulate sulfate (SO4f), NH_3, fine particulate ammonium (NH4f), HNO_3, fine particulate nitrate (NO3f), HCl, and fine particulate chloride (CLf) for winter (December, January, and February (DJF)) 2001 between MAM_CON and MAM_CON/ISO. Figure S2 shows the distributions of TCAT/TSO4 in MAM_CON and MAM_CON/ISO, and their absolute differences for summer and winter, 2001. In summer, as shown in Figure 6 in the paper, compared to MAM_CON, TCAT/TSO4 in MAM_CON/ISO either increases up by 80.1 (mostly over ocean) or decreases up by 51.8 (over both land and ocean), leading to a net increase of 0.7. In MAM_CON, most regions are in sulfate-poor regime, whereas Greenland, southeast U.S., North Africa, a small portion of Asia and North Atlantic Ocean, and some areas in North Pole are in sulfate-rich regime in summer. However, due to the simplified thermodynamics treatment in MAM_CON, NH_3 is underpredicted and NH_4^+ is overpredicted (see Table 3 in the paper). With the inclusion of ISORROPIA II, most sulfate-poor regions over land and over part of Pacific Ocean and most Atlantic Ocean become less sulfate-poor. The sulfate-poor regime can drive HNO_3/HCl to produce NO_3^-/Cl^- by neutralizing excess NH_4^+. If the amount of NO_3^-/Cl^- is insufficient to neutralize NH_4^+, sulfate-poor regime can drive NH_4^+ to the gas phase to produce NH_3. Therefore, the increase of NH_3 and decrease of NH_4^+ in MAM_CON/ISO are mainly due to insufficient NO_3^-/Cl^- to neutralize NH_4^+ under sulfate-poor regime. Insufficient NO_3^-/Cl^- results from the thermodynamic partitioning under higher temperature conditions that favors the production of HNO_3 and HCl from NO_3^-/Cl^- to produce HNO_3 and HCl under higher temperature conditions. The slight increase of NO_3^- over Pacific Ocean and South Atlantic Ocean is due to much higher Na^+ concentrations yet insufficient SO_4^{2-} in those regions compared with those over the land areas. Unlike a sulfate-poor regime, a sulfate-rich regime (e.g., small portion of North Atlantic Ocean, South China Sea, and Greenland), requires more cations such as NH_4^+ and Na^+ to neutralize excess SO_4^{2-} in the system and the thermodynamics favors the partitioning of volatile species such as NO_3^- and Cl^- in the gas phase as HNO_3 and HCl. Therefore, despite the increased temperatures, the decrease of NH_4^+ due to its evaporation back to the gas-phase is not as significant as that of NO_3^- and Cl^-, because NH_4^+ needs to stay in the system to neutralize SO_4^{2-}. In winter, as shown in Figure S1, compared with MAM_CON, the mixing ratios of H_2SO_4 in MAM_CON/ISO either increase by up to 4.3 ppt, or decrease by up to 1.0 ppt, leading to a net increase with the global mean of 0.001 ppt. NH_3 increases over most regions except Europe, eastern China, and some regions in North Pole. HNO_3 decreases over most oceanic areas, Northeastern China, and East Europe, whereas increases over South Asia, North Pole, southern U.S., Africa, and most land areas in southern hemisphere. HCl increases over most areas except the northeastern portion of Asia and eastern Europe.

Compared with MAM_CON, MAM_CON/ISO predicts higher HNO_3 and HCl over some land areas. As shown in Figure S2, in MAM_CON, most regions are in sulfate-poor regime, whereas Greenland, North Pole, North Africa, some portions of Asia and western Pacific Ocean are in sulfate-rich regime. For example, northeastern China is in sulfate-poor regime, driving HNO_3 and HCl partitioning to the aerosol phase to neutralize excess NH_4^+. This results in an increase in NO3f and Clf, changing sulfate-poor regime to less sulfate-poor. North Pacific Ocean and southern oceanic areas are also in sulfate-poor regime, and the increase of NO3f is due to the partitioning HNO_3 to the aerosol phase to neutralize Na^+, whose concentration is relatively higher compared to that over land areas. Therefore, more anions such as NO_3^- are needed to neutralize the system. However, the decrease Cl^- over these regions is due to the equilibrium state of HCl under different atmospheric conditions. The western Pacific Ocean is in sulfate-rich regime, driving NO_3^- and Cl^- partition to the gas phase, which results in a decrease in NO3f and Clf, and an increase in HNO_3 and HCl over this region. With the inclusion of ISORROPIA II, the western Pacific Ocean changes from sulfate-rich regime to less sulfate-rich regime.

Figure S3 shows the absolute differences of major inorganic gas and aerosol species between metastable (MAM_NEWA) and stable (MAM_NEWB) conditions. Compared with MAM_NEWA, the global average changes predicted by MAM_NEWB are overall small (within 5%) for most gaseous and aerosol species. For example, the global average changes are 0.01 μg m^{-3} (by 4.2%) for SO_4^{2-}, 0.005 μg m^{-3}(by 12.8%) for NH_4^+, 0.006 μg m^{-3}(by -0.01%) for NO_3^-, and -4×10^{-4} μg m^{-3} (by 2.0%) for Cl^-. The increase of SO_4^{2-} results in an increase in NH_4^+ (e.g., East Asia and Northeast U.S.). The differences between stable and metastable conditions may be more significant under low RH conditions (RH < 50% for nitrate, Fountoukis et al., 2009). However, based on the simulated global annual mean RH values, most regions have RH values >

60-70% (exceptions are over desert/arid regions such as Australia, the northern Africa, Arabian Desert, northwestern China, and western U.S.). These results indicate that the assumption of metastable conditions is not a significant sources of uncertainty for global model predictions of gaseous and aerosol species.

5. Impact of New and Modified Treatments on JJA Average Results from the 2001-2005 Simulations

Figure S4 shows the absolute differences of surface SO_2, NH_3, SO_4^{2-}, NH_4^+, TC, $PM_{2.5}$, PM_{10}, J, and PM_{num} and Figure S5 shows the absolute differences of cloud and radiative variables between MAM_SIM_5Y and MAM_NEW_5YA for JJA average of 2001-2005. Compared with MAM_SIM_5Y, MAM_NEW_5YA predicts lower SO_2 and NH_3 over East Asia with higher SO_4^{2-} and NH_4^+ in this region. More SO_2 is oxidized to form SO_4^{2-}, leading to enhanced acidity, which drives more NH_3 partitioning into NH_4^+ to neutralize the system in this region. SO_4^{2-} decreases over CONUS whereas NH_4^+ increases, driving more HNO_3 and HCl partitioning into NO_3^- and Cl^- to neutralize NH_4^+. Therefore, the concentrations of $PM_{2.5}$ and PM_{10} increase over CONUS. The overprediction of NH_4^+ over Europe and CONUS is mainly due to additional anions (NO_3^- and Cl^-) in the system, leading to perturbations in the thermodynamic equilibrium. Similar to Figure 7 in the paper, J and PM_{num} increase near the surface, resulting in an increase in AOD and cloud variable predictions such as column CCN5, CDNC, and COT (see Figure S5). As shown in Figure S5, SWD decreases by 3.2 W m^{-2} in global mean, which is due to the increased cloud predictions (e.g., column CCN5, CDNC, and COT). Due to aerosol direct and indirect effects, SWCF increases by 2.6 W m^{-2} in global mean. Compared with ANU, the absolute change of most radiative variables are smaller in JJA. The absolute changes of PM_{10} are larger in ANU than in JJA, which is mainly due to the dust events during other months (e.g., March-May over East Asia).

Table S1. Datasets for model evaluation

Species/Variables	Dataset
Downwelling longwave radiation (LWD)	BSRN
Downwelling shortwave radiation (SWD)	BSRN
Outgoing longwave radiation (OLR)	NOAA/CDC
Cloud fraction (CF)	MODIS
Cloud optical thickness (COT)	MODIS
Cloud water path (CWP)	MODIS
Precipitating water vapor (PWV)	MODIS
Aerosol optical depth (AOD)	MODIS
Column cloud condensation nuclei (ocean) at S = 0.5% (CCN5)	MODIS
Cloud droplet number concentration (CDNC)	BE07
Shortwave cloud radiative forcing (SWCF)	CERES
Carbon monoxide (CO)	East Asia: NIES of Japan, TAQMN
Ozone (O_3)	CONUS: CASTNET Europe: Airbase, BDQA, EMEP East Asia: TAQMN
Sulfur dioxide (SO_2)	CONUS: CASTNET Europe: Airbase, BDQA, EMEP East Asia: MEP of China, NIES of Japan, TAQMN
bNitric acid (HNO_3)	CONUS: CASTNET Europe: EMEP
Ammonia (NH_3)	Europe: Airbase, EMEP
Nitrogen dioxide (NO_2)	Europe: Airbase, BDQA, EMEP East Asia: NIES of Japan, TAQMN
Sulfate (SO_4^{2-})	CONUS: CASTNET, IMPROVE, STN Europe: Airbase, EMEP
Ammonium (NH_4^+)	CONUS: CASTNET, IMPROVE, STN Europe: Airbase, EMEP
Nitrate (NO_3^-)	CONUS: CASTNET, IMPROVE, STN Europe: Airbase, EMEP
Chloride (Cl^-)	CONUS: IMPROVE Europe: Airbase, EMEP
Organic carbon (OC), Black carbon (BC), Total carbon (TC)	CONUS: IMPROVE, STN
Particulate matter with diameter less than 2.5 μm ($PM_{2.5}$)	CONUS: IMPROVE, STN Europe: BDQA, EMEP
Particulate matter with diameter less than 10 μm (PM_{10})	Europe: Airbase, BDQA, EMEP East Asia: MEP of China, NIES of Japan, TAQMN
Column CO	Globe: MOPITT
Column NO_2	Globe: GOME
Tropospheric ozone residual (TOR)	Globe: TOMS/SBUV
New particle formation rate (J)	Globe: Kulmala et al. (2004); Yu et al. (2008)

BSRN: Baseline Surface Radiation Network; NOAA/CDC: National Oceanic and Atmospheric Administration Climate Diagnostics Center; MODIS: Moderate Resolution Imaging Spectroradiometer; BE07: Bennartz, 2007; CERES: Clouds and Earth's Radiant Energy System; TOMS/SBUV: the Total Ozone Mapping Spectrometer/the Solar Backscatter UltraViolet; MOPITT: the Measurements Of Pollution In The Troposphere; GOME: Global Ozone Monitoring Experiment; CASTNET: Clean Air Status and Trends Network; IMPROVE: Interagency Monitoring of Protected Visual Environments; STN: Speciation Trends Network; EMEP: European Monitoring and Evaluation Program; BDQA: Base de Données sur la Qualité de l'Air; AirBase: European air quality database; MEP of China: Ministry of Environmental Protection of China; TAQMN: Taiwan Air Quality Monitoring Network; NIES of Japan: National Institute for Environmental Studies of Japan.

Table S2. Probability of differences in Radiative/Cloud Predictions between Paired-Simulation

Species/Variables	Paired-simulation					
	MAM_SIM/ MAM_CB05_GE	MAM_CB05_GE/ MAM_CON	MAM_CON/ MAM_CON/IMN	MAM_CON/ MAM_CON/ISO	MAM_SIM/ MAM_NEWA	MAM_NEWA/ MAM_NEW/EMIS
LWD	0.7	0.6	0.2	0.8	0.5	0.7
SWD	8.1×10^{-3}	0	0.03	5.1×10^{-12}	1.3×10^{-12}	0.3
OLR	4×10^{-4}	0	0.9	1.6×10^{-10}	4.6×10^{-13}	0.8
SWCF	2×10^{-4}	1.2×10^{-12}	0.4	0	5.7×10^{-12}	0.2
CF	8.7×10^{-5}	1.2×10^{-12}	0.05	5.3×10^{-12}	0	0.4
COT	2.3×10^{-3}	0	3.9×10^{-3}	1.5×10^{-12}	2.3×10^{-12}	0.3
CWP	3.7×10^{-3}	0	0.06	5.4×10^{-12}	6.8×10^{-13}	0.2
PWV	0.4	0.08	0.5	0.1	0.2	0.9
AOD	7.9×10^{-5}	0	3.1×10^{-6}	3.8×10^{-13}	1.8×10^{-11}	0.03
Column CCN5 (ocean)	5.3×10^{-12}	0	3.3×10^{-12}	0	0	0
CDNC	2.7×10^{-10}	2.6×10^{-12}	9.8×10^{-9}	0	6.4×10^{-13}	0.5

*Probability value is expressed in fraction, with a minimum value of 0 and a maximum value of 1. A value less than 0.05 (i.e., 5%) indicates that the differences between the simulation pairs are statistically significant at the 95% confidence level.

Table S3. Statistical Performance of Radiative/Cloud Predictions during JJA, 2001-2005

Species/Variables	**Dataset**	**Obs**	**Simulations**		
			MAM_SIM_5Y	**MAM_NEW _5YA**	**MAM_NEW _5YB**
LWD (W m^{-2})	CERES	320.3	317.3/-3.0/-0.9/3.0/13.0[a]	318.0/-2.3/-0.7/3.0/12.8	318.1/-2.2/-0.7/2.9/12.6
SWD (W m^{-2})	CERES	192.4	197.9/5.5/2.9/9.7/25.1	194.1/1.7/0.9/9.5/24.3	196.2/3.8/2.0/9.5/23.6
OLR (W m^{-2})	NOAA-CDC	220.6	227.0/6.4/2.9/4.4/11.8	224.9/4.3/2.0/4.0/11.1	224.9/4.3/2.0/4.0/11.1
SWCF (W m^{-2})	CERES	-41.3	-40.1/1.2/-2.8/-25.9/16.4	-42.8/-1.5/3.6/-26.4/16.6	-41.2/0.1/-0.3/-26.3/16.2
CF (%)	MODIS	69.9	65.3/-4.6/-6.5/13.7/12.5	66.0/-3.9/-5.6/13.0/12.2	65.5/-4.4/-6.3/13.6/12.3
COT	MODIS	17.1	8.5/-8.6/-50.6/65.1/14.9	9.4/-7.7/-45.0/60.7/14.5	9.0/-8.1/-47.5/60.0/14.1
CWP (g m^{-2})	MODIS	87.9	41.7/-46.2/-52.6/53.3/54.5	47.2/-40.7/-46.3/47.4/50.7	46.6/-41.3/-47.0/47.8/51.4
PWV (cm)	MODIS	2.1	2.1/0.05/2.4/12.8/36.0	2.1/0.07/3.2/12.1/34.2	2.1/0.01/0.6/13.2/37.0
AOD	MODIS	0.2	0.2/-0.06/-34.1/54.5/0.2	0.2/-0.05/-29.0/51.3/0.2	0.2/-0.04/-25.0/48.7/0.2
Column CCN5 (ocean) (cm^{-2})	MODIS	2.3×10^{8}	6.1×10^{7}/-1.7×10^{8}/ -74.2/74.7/2.6×10^{8}	9.1×10^{7}/-1.4×10^{8}/ -59.8/61.9/2.3×10^{8}	9.1×10^{7}/-1.4×10^{8}/ -60.2/62.0/2.3×10^{8}
CDNC (cm^{-3})	BE07	117.4	48.5/-68.9/-58.8/61.1/87.7	69.5/-47.9/-40.8/49.7/76.2	67.7/-49.7/-42.3/50.8/77.1

[a] The values are expressed as Sim/MB/NMB/NME/RMSE, where Sim is modeled value; MB is mean bias; NMB is normalized mean bias (%); NME is normalized mean error (%); and RMSE is root mean square error.

Table S4. Statistical Performance of Chemical Predictions during JJA, 2001-2005

Variable[a]	Domain	Obs.	Simulations		
			MAM_SIM_5Y	MAM_NEW _5YA	MAM_NEW _5YB
CO	East Asia	535.4	-	119.4/-416.1/-77.7/77.7/441.1[b]	114.8/-420.6/-78.6/78.6/444.7
SO_2	CONUS	2.0	8.3/6.3/309.8/312.1/9.6	8.2/6.2/309.0/311.4/9.6	8.0/6.0/297.5/299.9/9.3
	Europe	5.3	6.0/0.7/12.4/85.2/7.1	6.0/0.7/13.3/87.3/7.3	6.3/1.0/19.2/90.1/7.5
	East Asia	3.7	2.3/-1.4/-37.2/57.6/2.5	3.2/-0.5/-12.6/59.2/3.5	3.2/-0.5/-14.9/58.0/3.6
NH_3	Europe	6.0	2.7/-3.2/-54.4/84.0/18.0	2.2/-3.8/-62.9/82.6/18.0	2.4/-3.5/-59.1/82.7/18.0
NO_2	Europe	18.5	-	4.2/-14.3/-77.4/78.2/17.8	4.4/-14.1/-76.4/77.3/17.6
	East Asia	13.2	-	2.1/-11.1/-84.2/84.2/12.1	2.1/-11.1-84.5/84.5/12.1
O_3	CONUS	39.4	-	47.4/8.0/20.2/23.9/11.7	46.9/7.5/19.2/22.9/11.2
	Europe	64.9	-	93.8/28.9/44.5/44.6/32.0	96.2/31.3/48.2/48.3/34.4
	East Asia	21.7	-	34.2/12.5/57.5/57.5/13.7	33.9/12.2/56.4/56.4/13.3
HNO_3	CONUS	1.6	-	1.8/0.2/10.5/40.9/0.9	1.6/0.04/2.5/38.7/0.8
	Europe	1.0		1.8/0.8/87.4/118.0/1.3	1.9/0.9/94.8/125.8/1.4
SO_4^{2-}	CONUS	3.6	3.2/-0.5/-12.4/22.1/1.1	3.2/-0.4/-10.3/19.9/1.0	3.1/-0.5/-12.7/19.1/0.9
	Europe	2.4	2.9/0.5/20.5/46.7/1.6	2.8/0.4/17.4/42.2/1.5	2.9/0.5/22.0/44.7/1.5
NH_4^+	CONUS	1.3	1.3/-0.02/-1.3/20.2/0.4	1.4/0.1/9.8/31.8/0.6	1.4/0.1/11.0/28.1/0.5
	Europe	0.8	1.0/0.2/30.3/46.8/0.6	1.6/0.8/95.0/99.7/1.1	1.6/0.8/96.0/100.6/1.1
NO_3^-	CONUS	0.5	-	0.7/0.2/37.8/84.5/0.6	0.8/0.3/57.1/97.9/0.7
	Europe	1.3	-	1.5/0.3/22.0/55.1/1.0	1.5/0.3/26.5/52.2/1.0
Cl^-	CONUS	0.1	-	0.1/-4.0×10^{-3}/-5.3/98.5/0.2	0.1/-4.0×10^{-3}/-5.4/101.2/0.2
	Europe	0.1		1.1/1.0/650.0/650.0/1.4	1.1/1.0/666.8/666.8/1.4
BC	CONUS	0.4	0.4/-0.02/-5.0/42.3/0.2	0.4/-0.02/-4.8/42.3/0.2	0.4/-0.02/-5.7/41.3/0.2
OC	CONUS	1.7	1.1/-0.6/-34.8/50.5/1.1	1.5/-0.2/-13.6/50.6/1.1	1.4/-0.3/-15.6/45.9/1.0
TC	CONUS	3.5	1.5/-1.9/-55.8/60.0/2.5	2.1/-1.4/-40.6/49.7/2.2	2.0/-1.5/-42.8/50.3/2.2
$PM_{2.5}$	CONUS	10.6	8.4/-2.2/-20.5/35.5/4.9	10.0/-0.6/-5.6/27.0/4.1	9.9/-0.7/-6.3/19.4/2.6
	Europe	13.1	8.7/-4.4/-33.6/34.8/5.4	10.1/-3.0/-23.0/30.4/5.0	11.9/-1.1/8.7/26.1/4.3
PM_{10}	Europe	25.9	16.4/-9.5/-36.6/41.4/12.5	18.3/-7.6/-29.4/34.5/11.7	21.6/-4.3/-16.7/26.6/9.7
	East Asia	85.4	31.5/-54.0/-63.2/65.0/59.0	39.9/-45.6/-53.3/54.6/51.2	45.4/-40.0/-46.8/51.3/48.4
Col.CO	Globe	1.3×10^{18}	-	1.2×10^{18}/-1.1×10^{17}/-8.2/26.8/4.4×10^{17}	1.2×10^{18}/-1.3×10^{17}/-10.0/28.1/4.7×10^{17}
Col.NO_2	Globe	5.9×10^{14}	-	9.0×10^{14}/3.1×10^{14}/52.2/65.0/5.2×10^{14}	8.8×10^{14}/2.9×10^{14}/48.9/62.4/5.1×10^{14}
TOR	Globe	32.1	29.8/-2.3/-7.4/18.9/6.9	31.1/-1.0/-3.0/14.2/5.9	30.4/-1.7/-5.4/15.4/6.2

[a]The units are CO, ppm (over East Asia); SO_2, ppb (over East Asia) and μg m^{-3} (over CONUS); O_3, ppb (over CONUS) and μg m^{-3} (over Europe); column CO and NO_2, molecules cm^{-2}; TOR, DU. All other concentrations are in μg m^{-3}.

[b]The values are expressed as Sim/MB/NMB/NME/RMSE, where Sim is modeled value, MB is mean bias; NMB is normalized mean bias (%); NME is normalized mean error (%); RMSE is root mean squared error.

MAM_CON/ISO - MAM_CON

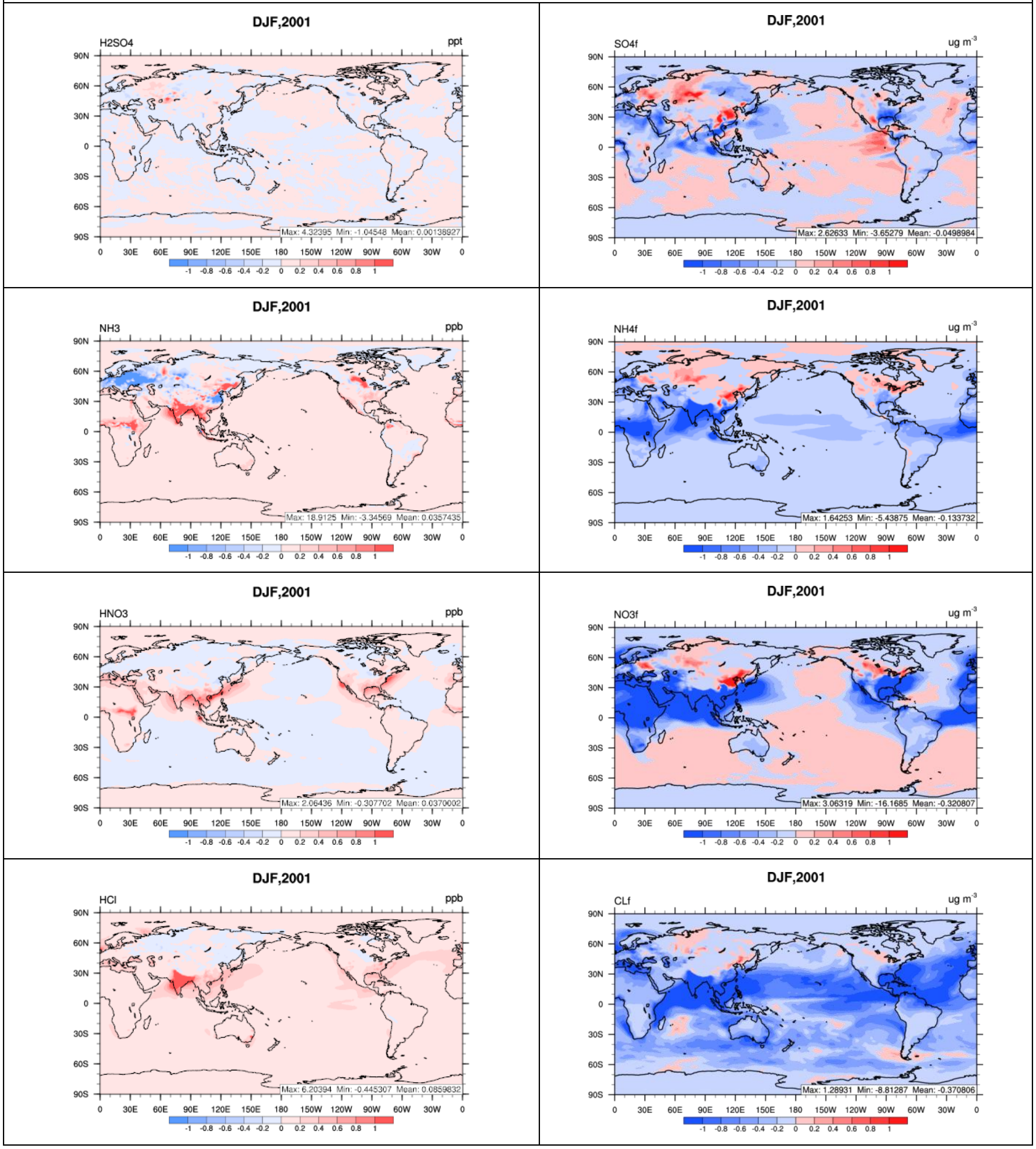

Figure S1. Absolute differences of major PM species and their gas precursors between MAM_CON/ISO and MAM_CON for winter, 2001.

	JJA, 2001	**DJF, 2001**
MAM_CON	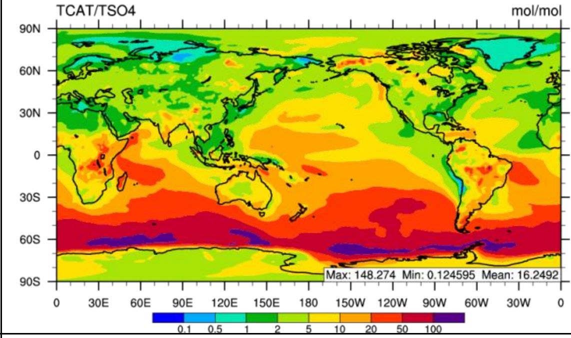	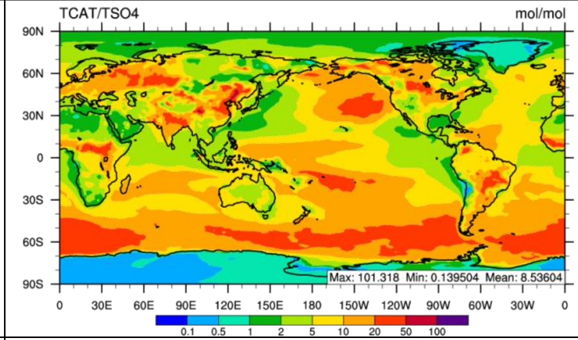
MAM_CON/ISO	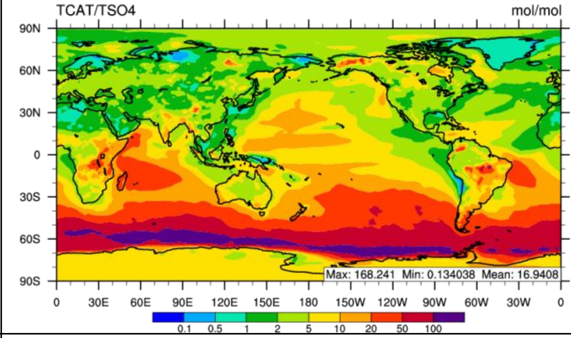	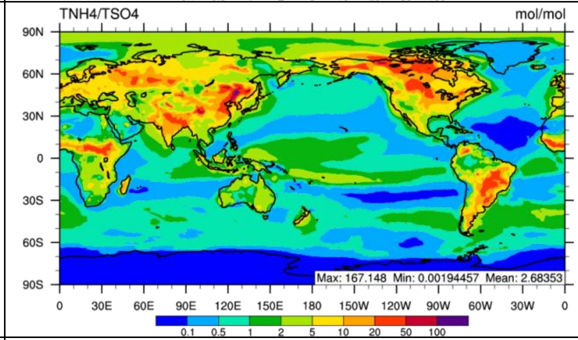
MAM_CON/ISO - MAM_CON	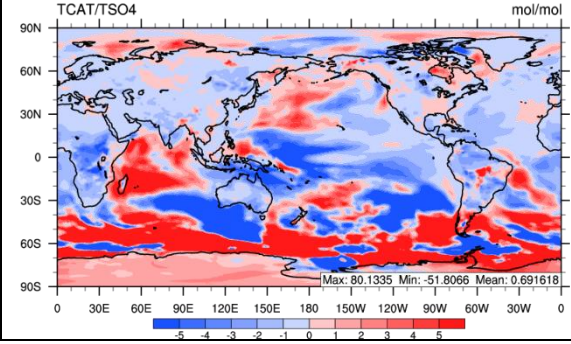	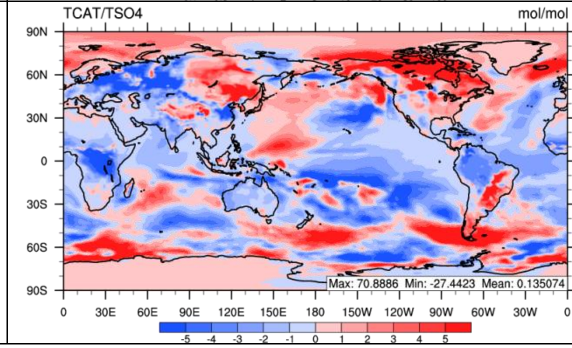

Figure S2. Surface distribution of TCAT/TSO4 in MAM_CON and MAM_CON/ISO and absolute differences of TCAT/TSO4 between MAM_CON/ISO and MAM_CON for summer and winter, 2001

MAM_NEWB – MAM_NEWA

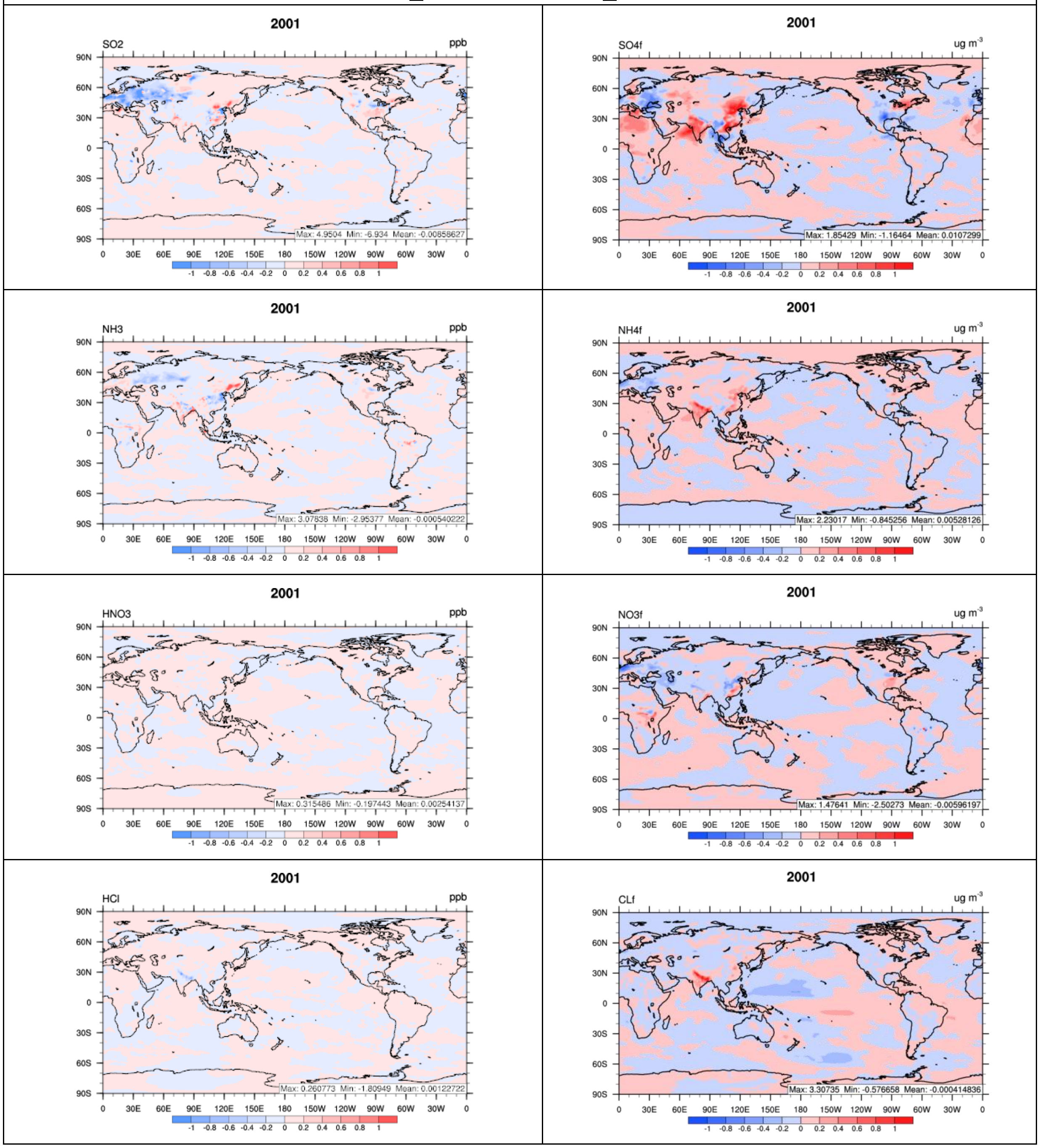

Figure S3. Absolute differences of major aerosol species and their gas precursors between metastable and stable conditions.

MAM_NEW_5YA – MAM_SIM_5Y (JJA, 2001-2005)

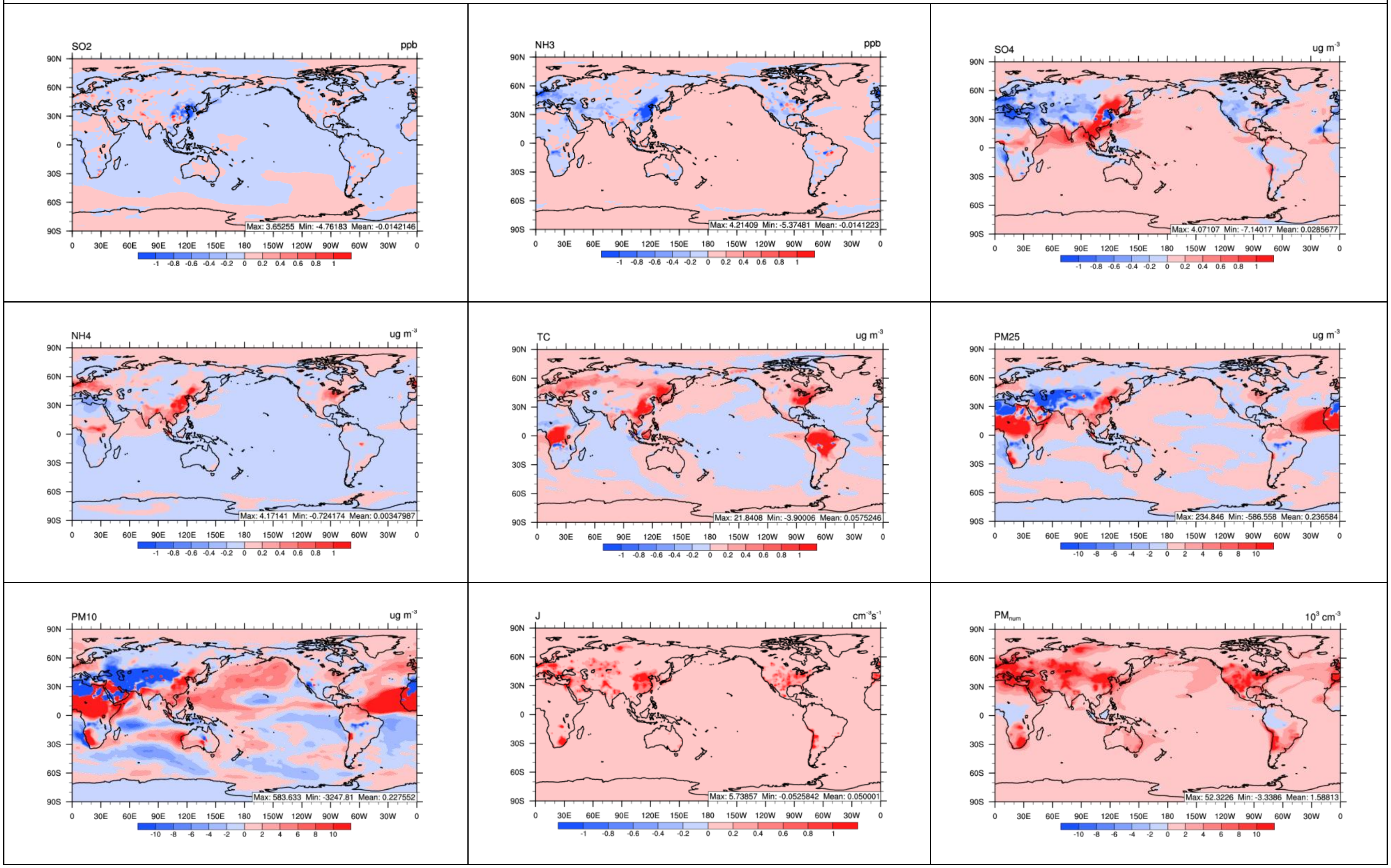

Figure S4. Absolute differences of major aerosol species and their gas precursors, new particle formation rate (J), and aerosol number between MAM_NEW_5YA and MAM_SIM_5Y for June, July, and August (JJA), 2001-2005.

MAM_NEW_5YA – MAM_SIM_5Y (JJA, 2001-2005)

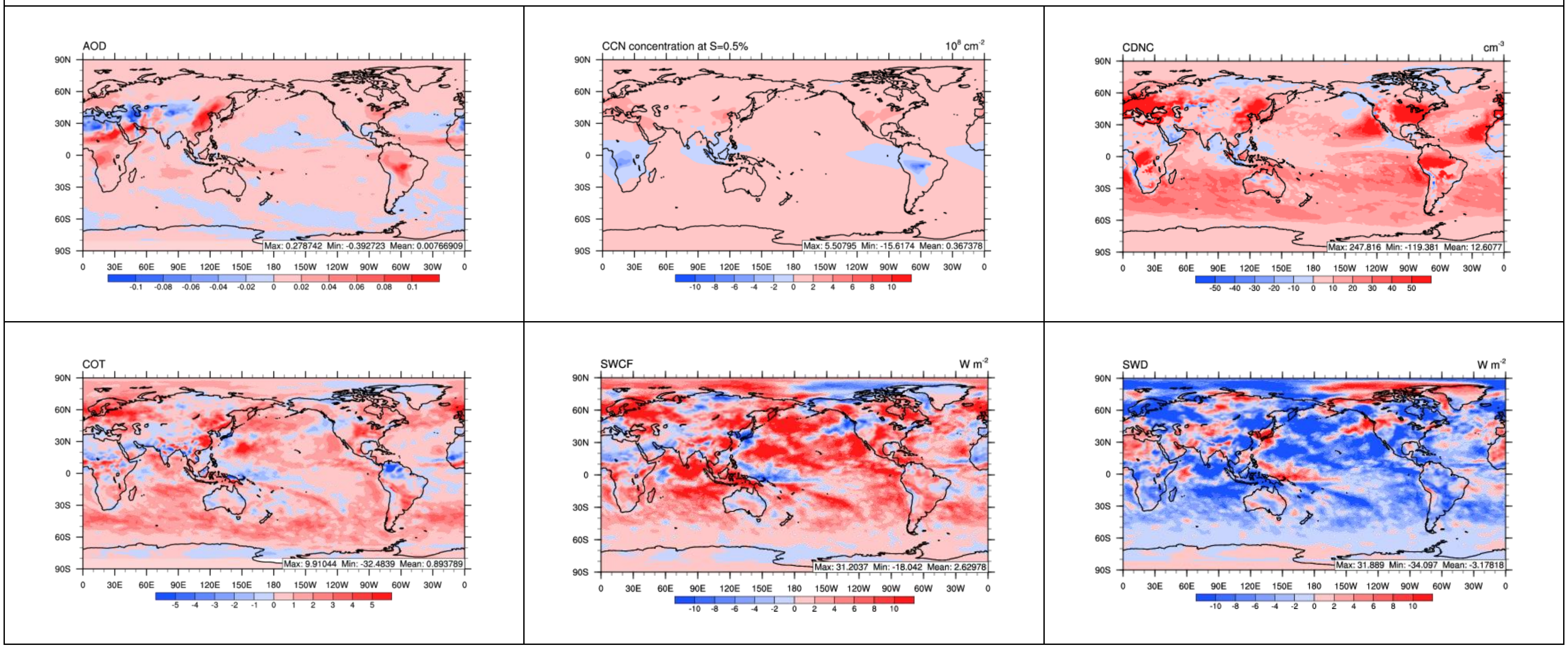

Figure S5. Absolute differences of major cloud and radiative variables between MAM_NEW_5YA and MAM_SIM_5Y for June, July, and August (JJA), 2001-2005.

References:

Fountoukis, C., Nenes1, A., Sullivan, A., Weber, R., Farmer, D., and Cohen, R. C., 2009, Thermodynamic characterization of Mexico City aerosol during MILAGRO 2006, Atmos. Chem. Phys., 9, 2141-2156, 2009.

Kulmala, M., Vehkamaki, H., Petaja, T., Dal Maso, M., Lauri, A., Kerminen, V.-M., Birmili, W., and McMurry, P.: Formation and growth rates of ultrafine atmospheric particles: A review of observations, J. Aerosol Sci., 35, 143-176, 2004.

Yu, F., Wang, Z., Luo, G., and Turco, R. P.: Ion-mediated nucleation as an important global source of tropospheric aerosols, Atmos. Chem. Phys., 8, 2537-2554, 2008.

Zhang, Y., Seigneur, C., Seinfeld, J. H., Jacobson, M., Clegg, S. L., Binkowski, F. S.: A comparative review of inorganic aerosol thermodynamic equilibrium modules: similarities, differences, and their likely causes, Atmos. Environ., 34, 117-137, 2000.